Generalized Equation for Soil Shrinkage Curve

Pan Chen[1] and Ning Lu, F.ASCE[2]

Abstract: The soil shrinkage curve (SSC) defines a constitutive relationship between soil volume and water content under drying conditions. Nearly all work to date considers a zero volume shrinkage for water content below a certain value such as shrinkage limit, which contradicts some recent experimental evidence of pervasive nonzero shrinkage for clayey soils. This paper uses a soil-water retention (SWR)-based conception to theorize such nonzero shrinkage behavior by considering the mechanical effect of capillary and adsorptive SWR mechanisms. A mathematical equation for SSC in the full water content range is developed, which conceptualizes a linear relation for adsorption shrinkage and a sigmoid relation for capillary shrinkage. The equation is validated with test data for a variety of soils. For given soils, the maximum adsorption water contents inferred independently from the SWR and SSC data are highly correlated, with a factor of 2.47. The analysis shows that the adsorption shrinkage rate is strongly correlated with the SWR characteristics of specific surface area (SSA) and cation exchange capacity (CEC). A universal exponential form between the adsorption shrinkage rate and SSA and between the adsorption shrinkage rate and CEC is discovered for silty and clayey soils. **DOI: 10.1061/(ASCE)GT.1943-5606.0001889.**

Author keywords: Soil shrinkage; Clayey soil; Adsorption water; Capillarity; Shrinkage rate; Unsaturated soil.

Introduction

The soil shrinkage curve (SSC) defines a constitutive relationship between void ratio and water content under free external stress conditions from a fully saturated state to a completely dry state (e.g., Tempany 1917; Haines 1923; Mitchell 1992). SSC has been considered as one of the most important constitutive relationships or characteristic curves like the soil-water retention curve (SWRC) to describe mechanical and hydraulic behavior of unsaturated soils (e.g., Crescimanno and Provenzano 1999; Boivin et al. 2006). It plays an important role in understanding the mechanism of soil-water interaction and assessing soil deformation behaviors, especially for clayey soils (e.g., Chertkov 2003). For example, it has been widely used to quantify the indices of soil structure (e.g., McGarry and Daniells 1987). Because of the importance of the soil shrinkage characteristics, numerous workers have studied the soil shrinkage behavior (e.g., Sridharan and Rao 1971; Kim et al. 1992; Braudeau et al. 1999; Zolfaghari et al. 2016). The existing knowledge shows that soil shrinkage has a very significant effect on soil mechanical and hydraulic properties such as the air-entry value of soils (e.g., Wijaya et al. 2015), wilting point and field capacity (e.g., Braudeau et al. 2005), water and air permeability (e.g., Millette and Broughton 1984), and Young's modulus (e.g., Dong and Lu 2017).

SSC is generally divided into four characteristic stages in the literature: structural (undisturbed field conditions) shrinkage, proportional shrinkage, residual shrinkage, and zero shrinkage (e.g., Peng and Horn 2005; Cornelis et al. 2006). The common definition for the zero-shrinkage state is that soil volume remains constant when the water content further decreases. However, this is not always the case, especially for clayey soils. Further change of soil volume has been observed in soil shrinkage experiments, for instance, a decrease in volume for expansive clays (e.g., McGarry and Malafant 1987; Boivin et al. 2006) and clay soil (e.g., Olsen and Haugh 1998) as the water content further decreases under drying conditions. Furthermore, SSC cannot always be classified by the four-stage methodology for all soils. One or more shrinkage stages of soils may be absent during drying processes. According to their investigation of the measured database of soil shrinkage, Peng and Horn (2013) identified six types of SSC, in which zero, one, two, or three shrinkage stages can be absent.

Many empirical equations have been proposed to characterize the SSC. Based on the geometry of the measured SSC, different mathematical equations have been developed to describe SSC (e.g., McGarry and Malafant 1987; Tariq and Durnford 1993; Braudeau et al. 1999). Initially, three straight lines were adopted to simply portray three shrinkage stages of SSC (McGarry and Malafant 1987). Tariq and Durnford (1993) further developed a polynomial equation in which four shrinkage stages were modeled by two linear and two polynomial curves separated by three transition points. Braudeau et al. (1999) used an exponential equation to cover the entire shrinkage curve, in which five shrinkage zones need to be characterized by three linear and two exponential curves separated by four transition points. Leong and Wijaya (2015) suggested that several linear segments and curvilinear segments between linear segments can be used to describe SSC with different shrinkage stages. Although these equations have been shown to fit experimental data well (e.g., Tariq and Durnford 1993; Braudeau et al. 1999; Boivin et al. 2004, 2006; Leong and Wijaya 2015), these multiequation methods require that different parameters are defined, and most of them have little physical meaning. In general, the classification for the soil shrinkage behavior in these equations makes the shrinkage process complicated (Peng and Horn 2013).

Considering the hyperbolic nature of SSC without including the structural shrinkage stage, Fredlund et al. (2002) proposed one equation to describe the entire SSC. Noticing the geometric similarity between typical SSC and SWRC, Peng and Horn (2005) adopted a closed form of the modified van Genuchten (1980) SWR

[1]Associate Professor, State Key Laboratory of Geomechanics and Geotechnical Engineering, Institute of Rock and Soil Mechanics, Chinese Academy of Sciences, Wuhan, Hubei 430071, P.R. China. Email: pchen@whrsm.ac.cn

[2]Professor, Dept. of Civil and Environmental Engineering, Colorado School of Mines, Golden, CO 80401 (corresponding author). Email: ninglu@mines.edu

Note. This manuscript was submitted on December 27, 2016; approved on December 12, 2017; published online on May 24, 2018. Discussion period open until October 24, 2018; separate discussions must be submitted for individual papers. This paper is part of the ***Journal of Geotechnical and Geoenvironmental Engineering***, © ASCE, ISSN 1090-0241.

equation to mimic SSC. The equation has been assessed using the shrinkage data of different soils and was shown to be capable of fitting the measured data well for a variety of soils (e.g., Peng and Horn 2005; Boivin et al. 2006; Peng and Horn 2013).

Soil-water interactions involve two physical mechanisms: capillarity and adsorption. At high water content, capillary water plays a dominant role in soil shrinkage (e.g., Lu and Khorshidi 2015). As drying proceeds, capillary water diminishes and adsorptive water on particle surfaces could be active in soil shrinkage. Further drying may cause an onset of dehydration of exchangeable cations when gravimetric water content is less than ~10% or matric suction is higher than a few hundred MPa (Lu and Khorshidi 2015). A reduction of water content under such low water content conditions will result in a reduction of crystalline volume with a certain value of shrinkage rate, which contradicts the zero-shrinkage state in all traditional shrinkage classifications. Lu and Dong (2017) unambiguously observed the nonzero state in a variety of soils in the laboratory. However, the zero-shrinkage rate has been widely adopted in most of the soil shrinkage models (e.g., Tariq and Durnford 1993; Braudeau et al. 1999; Fredlund et al. 2002; Chertkov 2003; Peng and Horn 2005; Leong and Wijaya 2015). Although Kim et al. (1992) proposed a SSC equation with a nonzero shrinkage rate at zero-water content, the meaning of the constant shrinkage rate was not physically representative for adsorption because it was formulated as the slope of saturation line of the SSC equal to unity.

Although the linkage between the SSC and SWRC has been noticed (e.g., Peng and Horn 2005; Boivin et al. 2006; Assi et al. 2014), a SSC equation directly considering the effect of the adsorptive SWR interaction on soil deformation has not yet been developed. Based on some recent breakthroughs in conceptualizing soil-water interaction mechanisms (Lu and Khorshidi 2015; Khorshidi et al. 2017; Khorshidi and Lu 2017a, b), and combined advances in laboratory techniques in measuring SSC (e.g., Dong and Lu 2017), Lu and Dong (2017) proposed a conceptual model for SSC that conceptualized SSC into two regimes (capillary and adsorption), which correspond to the two SWR mechanisms of capillarity and adsorption.

This paper establishes a generalized SSC by (1) explicitly considering the effect of SWR mechanisms of capillarity and adsorption on the shrinkage behavior of clayey soil, and includes a nonzero shrinkage rate in the adsorption regime; (2) validating the proposed equation by using the measured shrinkage data for a variety of soils; and (3) exploring the linkage of the SSC and SWR characteristics.

New Conceptual Model for SSC

The literature typically describes SSC by portraying the void ratio as a function of the moisture ratio (e.g., Groenevelt and Bolt 1972; Kim et al. 1992; Olsen and Haugen 1998; Peng and Horn 2005). The void ratio e is defined as the ratio of the volume of voids V_v to the volume of solids V_s, and the moisture ratio θ is defined as the ratio of the volume of water V_w to the volume of solids V_s. Because the void ratio and the moisture ratio are both normalized by the same quantity V_s, a soil deviating from the line of equal void ratio and moisture ratio indicates that the soil is under unsaturated conditions. Therefore, the relationship between the void ratio and the moisture ratio is used herein to describe SSC.

In light of the recent experimental evidence of the mechanical effect of capillary and adsorption water on soil volume shrinkage, SSC is conceptually divided into two regimes, namely capillary and adsorption regimes (Fig. 1). The capillary regime has two different states or stages, saturated shrinkage (capillary) and unsaturated

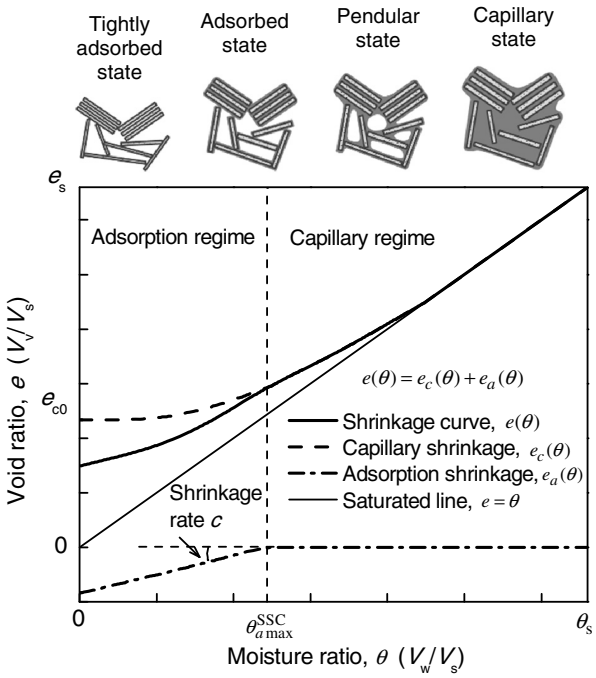

Fig. 1. Conceptual illustration of SSC for clayey soil.

shrinkage (pendular), due to the existence of the curved air-water interfaces. In the capillary state, a volume reduction in pore water results in an equal reduction in bulk soil volume. However, in the pendular state, a volume reduction in soil water will result in a lesser volume reduction in bulk soil, because part of the pore volume is replaced by air. In the adsorption regime, two states of soil shrinkage can be conceptualized, namely the adsorbed and tightly adsorbed states (Fig. 1). Lu and Khorshidi (2015) and Khorshidi and Lu (2017b) indicated that the adsorbed state is dominated by hydrated water on particle surface, and the tightly adsorbed state is controlled by hydrated water around the exchangeable cations. The tightly adsorbed state occurs at lower water content than that in the adsorbed state.

The boundary between the capillary and adsorption regimes for soil shrinkage can be defined by the maximum adsorption moisture ratio $\theta_{a\max}^{SSC}$ (Fig. 1). Thus, a complete SSC consists of two soil-water retention regimes including four shrinkage states, namely a capillary state, a pendular state, an adsorbed state, and a tightly adsorbed state, although some states may be missing in some soils, which may not be visually identified by the named shrinkage states.

As soil water further decreases from $\theta_{a\max}^{SSC}$, matric suction gradually increases to the soil water cavitation threshold (Lu 2016). A transition zone exists in which both capillary and adsorption shrinkages operate. The particle surface hydration or adsorption provided by van der Waals attraction becomes activated (e.g., Lu and Likos 2006), causing soil volume to continue shrinking. In the adsorbed state, the mechanical effect of soil water on soil shrinkage is less pronounced than that in the pendular state because most hydrated water on particle surfaces is away from the particle contacts. Accordingly, the shrinkage rate in this stage is generally much less than that in the pendular state (Fig. 1).

As soil water content further decreases, the capillary water eventually disappears and capillary shrinkage remains constant, and adsorption shrinkage dominates the soil shrinkage behavior. Dehydration of exchangeable cations is the sole mechanism of soil shrinkage in this tightly adsorbed state (Khorshidi and Lu 2017b) (Fig. 1). This state typically occurs in the range of gravimetric water content less than ~10% or matric suction higher than a few

hundred MPa (Lu and Khorshidi 2015; Khorshidi and Lu 2017b). In this stage, volumetric shrinkage occurs within crystalline clay minerals with a certain characteristic value of shrinkage rate upon a further reduction of water content. The adsorption shrinkage rate can be highly correlated with the physicochemical properties of a soil such as specific surface area (SSA) and cation exchange capacity (CEC) (Lu and Dong 2017). Therefore, for some silty and nonexpansive clays, a very low or nearly zero shrinkage rate is expected, due to low CEC, whereas clayey soils with strong cation hydration such as expansive clay will exhibit a pronounced shrinkage rate.

For simplicity, the current SSC model assumes a constant shrinkage rate in the adsorption regime, which is a good approximation to what Lu and Dong (2017) recently observed for different types of soils including silty and clayey soils. In contrast, the zero-shrinkage state commonly assumed in nearly all SSC models overlooks the physics of soil water hydration. The conceptual model herein generalizes the soil shrinkage behavior to include both capillary and adsorption mechanisms. Furthermore, the adsorption shrinkage rate is quantifiable and can be highly correlated with some SWR characteristics, such as SSA and CEC.

Generalized Equation for SSC

Based on the conceptual model in Fig. 1, the soil shrinkage curve $e(\theta)$ can be represented by two superimposable components, the change of adsorption shrinkage void ratio $e_a(\theta)$, and capillary shrinkage void ratio $e_c(\theta)$, respectively

$$e(\theta) = e_a(\theta) + e_c(\theta) \tag{1}$$

As a soil dries, the adsorption water starts to affect the soil's skeleton from the maximum adsorption moisture ratio $\theta_{a\max}^{\mathrm{SSC}}$ (Fig. 1). With the assumption of a constant shrinkage rate due to adsorption shrinkage, the change of adsorption shrinkage void ratio $e_a(\theta)$ is proposed

$$e_a(\theta) = \frac{1}{2}\left[1 - \mathrm{erf}\left(4\frac{\theta - \theta_{a\max}^{\mathrm{SSC}}}{\theta_{a\max}^{\mathrm{SSC}}}\right)\right] \times c(\theta - \theta_{a\max}^{\mathrm{SSC}}) \tag{2}$$

where $\theta_{a\max}^{\mathrm{SSC}}$ = maximum adsorption moisture ratio; c = adsorption shrinkage rate; and erf() = error function (e.g., Mathews and Walker 1970; Lu 2016), which is continuous in the range $[-\infty, +\infty]$. Hence, Eq. (2) gives a complete definition of the change of adsorption shrinkage void ratio even when $\theta < \theta_{a\max}^{\mathrm{SSC}}$, which is a closed form varying smoothly over the entire range of moisture ratio from the fully saturated to dry conditions (Fig. 1). The form of the error function ensures a smooth transition from zero adsorption shrinkage rate in the capillary shrinkage regime to a constant shrinkage rate c in the adsorption shrinkage regime crossing the maximum adsorption moisture ratio. The adsorption shrinkage rate c decreases to zero for most sandy and some silty soils, but remains a constant for clayey soils that can be characteristically correlated with the SWR characteristics of SSA and CEC.

For the capillary shrinkage, a sigmoid curve equation is adopted. Considering the effect of adsorption shrinkage, the following sigmoid form is proposed to describe the capillary shrinkage:

$$e_c = e_{c0} + (e_s - e_{c0} - e_a)\left[1 + \beta\frac{e_s - \theta}{\theta}\right]^{-\eta} \tag{3}$$

where e_s = saturated void ratio; e_{c0} = void ratio due to capillary shrinkage at zero water content; and β and η = fitting parameters. The moisture ratio θ ranges from 0 to the saturated moisture ratio θ_s. Because the volume of water equals the volume of pores in the fully saturated condition, the condition $\theta_s = e_s$ is true for any SSC. As such, the following physical constraint should be satisfied for any SSC:

$$\theta = \theta_s, \qquad e = e_s \tag{4}$$

Substituting $\theta = \theta_s$ into Eq. (3) leads to

$$\theta = \theta_s, \qquad e_c = e_s - e_a \tag{5}$$

Furthermore, substituting Eq. (5) into Eq. (1) shows that Eq. (4) is always held in the SSC Eq. (1).

Eqs. (1)–(3) completely define the proposed SSC equation with a total of six parameters: two in Eq. (2) for adsorption shrinkage, i.e., the adsorption shrinkage rate c within the adsorption regime and the maximum adsorption moisture ratio $\theta_{a\max}^{\mathrm{SSC}}$; and four in Eq. (3) for capillary shrinkage, i.e., the void ratio for capillary shrinkage e_{c0} at zero water content, saturated void ratio e_s, structural-related fitting parameter β, and capillary shrinkage rate–related fitting parameter η. The proposed SSC equation is capable of describing soil shrinkage behavior for both structural (undisturbed) and nonstructural (remolded or disturbed) soils. The listed parameters in the shrinkage equation are determined using the least-squares method by comparing the measured data and the data predicted by the equation. To avoid subjectivity, the Solver function in Microsoft Excel software was used for all fitting.

Assessments of Generalized SSC Equation

Shrinkage Curve Data

To validate the proposed SSC equation, the measured data for eleven soils from the literature were used, which range from silty to nonexpansive clayey to expansive clayey soils. Table 1 lists the geotechnical index and physicochemical properties of these soils.

These eleven soils were divided into four groups according to their characteristics and validation aspects. The soils in the first group were undisturbed or structural soils (Reeve and Hall 1978): Ragdale clay (poorly structured), and Faulkbourne Clay 1 (moderately structured) and Clay 2 (well-developed structure), respectively. A specific gravity of 2.65 g/cm^3 was assumed to convert the gravimetric water content to moisture ratio.

The soil shrinkage data in the second group were measured under the full saturation range including oven-dry state (Olsen and Haugen 1998). The soils were sampled from different depths: 0–20 cm (Norwegian Clay 1 with a clay-size content of 36%), and 20–40 cm (Norwegian Clay 2 with a clay-size content of 49%). The samples were saturated before the shrinkage experiment started.

The soil shrinkage data in the third group were determined from expansive clay from Prospect, New South Wales, Australia (Talsam 1977). Different pressures ($P = 0.0, 6.3$, and 11.2 kPa) were preloaded on saturated soil samples for consolidation prior to the shrinkage experiments.

The soil shrinkage data in the fourth group were measured in silty and clayey soil for both SWRC and SSC (Lu and Dong 2017). With the knowledge of SWR data, the role of adsorption and capillary water in soil shrinkage behavior can be examined. The SSCs for the five soils were measured (Lu and Dong 2017) by combining the drying cake technique (Lu and Kaya 2013) and low relative humidity control in laboratory (e.g., Dong and Lu 2017). The fully saturated soil samples were used in the test at the beginning. To prevent crack occurrence, a slow drying process was implemented.

Table 1. Geotechnical and physicochemical index properties of examined soils

Number	Soil	USCS classification	Porosity	CSC (%)	Surface properties		Atterberg limits		
					SSA (m^2/g)	CEC (meq/g)	LL (%)	PL (%)	PI (%)
1	Bonny silt[a]	ML	0.417	14	112	0.210	25	21	4
2	Iowa silt[a]	ML	0.458	10	104	0.220	33	24	9
3	BALT silt[a]	CL-ML	0.492	14	76	0.240	26	19	7
4	Ragdale clay[b]	N/A	0.452	44	N/A	0.424	N/A	N/A	N/A
5	Faulkbourne Clay 1[b]	N/A	0.459	44	N/A	0.411	N/A	N/A	N/A
6	Faulkbourne Clay 2[b]	N/A	0.456	36	N/A	0.462	N/A	N/A	N/A
7	Norwegian Clay 1[c]	N/A	0.470	36	N/A	N/A	N/A	N/A	N/A
8	Norwegian Soil 2[c]	N/A	0.490	49	N/A	N/A	N/A	N/A	N/A
9	Denver claystone[a]	CL	0.471	55	153	0.350	44	23	21
10	Prospect clay[d]	N/A	0.658	60	N/A	N/A	N/A	N/A	N/A
11	Denver bentonite[a]	CH	0.692	90	660	1.690	118	45	73

[a]Data from Khorshidi and Lu (2017a), SSA from Khorshidi et al. (2017), clay-size content (CSC) from Likos and Lu (2003), and Atterberg limit from Lu and Kaya (2014).
[b]Data from Reeve and Hall (1978).
[c]Data from Olsen and Haugen (1998).
[d]Data from Talsam (1977).

The particle image velocimetry (PIV) technique (e.g., White et al. 2003) was used to obtain the change of the diameter in the drying cake method by capturing digital images of the radial displacement field of a disk-shaped soil sample (Lu and Kaya 2013). Meanwhile, the water content of the sample was accurately recorded by an electronic balance (0.01 g). The drying cake method can provide an effective and accurate measurement of the deformation (±0.001 mm) of all types of soils (Lu and Kaya 2013; Dong and Lu 2017). Lu and Kaya (2013) and Dong and Lu (2017) provided details of the experimental techniques.

The following sections assess the ability of the proposed SSC equation to describe both structural and nonstructural soils, to define the maximum adsorption water content and its relation to that in the SWRC, to describe variety of soils, and to link soil shrinkage rate in the adsorption regime with the SWR characteristics.

Soil Shrinkage for Nonstructural and Structural Clayey Soils

The measured data and curves predicted by the proposed SSC Eqs. (1)–(3) were compared. The results showed that the least-squares fitted curves followed closely the measured data, with correlation coefficients R^2 larger than 0.98 (Table 2). Table 2 also lists the fitted parameters for the SSC equation. The results also demonstrated that the proposed SSC equation is capable of describing not only the shrinkage behavior of nonstructural clay [Ragdale clay, Fig. 2(a)] but also that of structural clay (Faulkbourne clay, Figs. 2(b and c)]. A strong dependence between the adsorption shrinkage rate and cation-exchange capacity of these three clays was observed (Tables 1 and 2). The correlation between the adsorption shrinkage rate and physicochemical indexes was further assessed subsequently with other soils.

Because of the significant clay contents, it was expected that adsorption shrinkage would be present, leading to nonzero adsorption shrinkage rates in the low moisture ratio range, although the SSC tests on these soils were terminated at moisture ratios greater than 0.15. The proposed SSC equation predicted the nonzero shrinkage state even though shrinkage data were absent in the low moisture ratio range for these clayey soils (Fig. 2). Furthermore, the results indicated that the adsorption shrinkage can provide a significant contribution to the overall soil shrinkage (Fig. 2). Hence, if the final deformation at near-zero moisture content is a concern, the SSC equation can give a quantitative evaluation of the final deformation. On the other hand, most existing SSC models would predict zero shrinkage in the low moisture ratio, leading to overestimation of the void ratio in the completely dry state.

Fig. 3 compares the measured data from Olsen and Haugen (1998) and the predicted curves from the proposed SSC model. High correlation coefficients R^2 larger than 0.98 (Table 2) were also obtained between the least-squares fitted curves and the measured data. Shrinkage rates of 0.140 and 0.105 obtained under full saturation including the oven-dry state were identified. Similar values (0.217 and 0.208) of the maximum adsorption moisture ratio $\theta_{a\max}^{SSC}$ for the two soils were obtained. Table 2 lists the fitted parameters for the SSC equation.

The preceding modeling for five nonstructural and structural clayey soils indicates that the proposed SSC model can accurately describe the shrinkage behavior.

Table 2. Fitted model parameters for proposed SSC equation and corresponding coefficients of correlation for examined clayey soils

Soil	e_s	e_{c0}	β	η	c	$\theta_{a\max}^{SSC}$	R^2
Ragdale clay	0.825	0.347	0.02	90.03	0.184	0.207	1.00
Faulkbourne Clay 1	0.850	0.445	0.03	45.45	0.145	0.171	0.99
Faulkbourne Clay 2	0.837	0.453	0.01	77.78	0.179	0.138	0.99
Norwegian Clay 1	1.100	0.821	0.002	734.2	0.140	0.217	0.98
Norwegian Clay 2	1.150	0.701	0.002	961.3	0.105	0.208	0.99
Prospect clay, $P = 0.0$	1.920	1.375	0.755	2.057	0.177	0.849	0.99
Prospect clay, $P = 6.3$	1.670	1.295	0.054	27.669	0.220	0.855	1.00
Prospect clay, $P = 11.2$	1.490	1.177	0.093	17.576	0.235	0.859	1.00

J. Geotech. Geoenviron. Eng., 2018, 144(8): 04018046

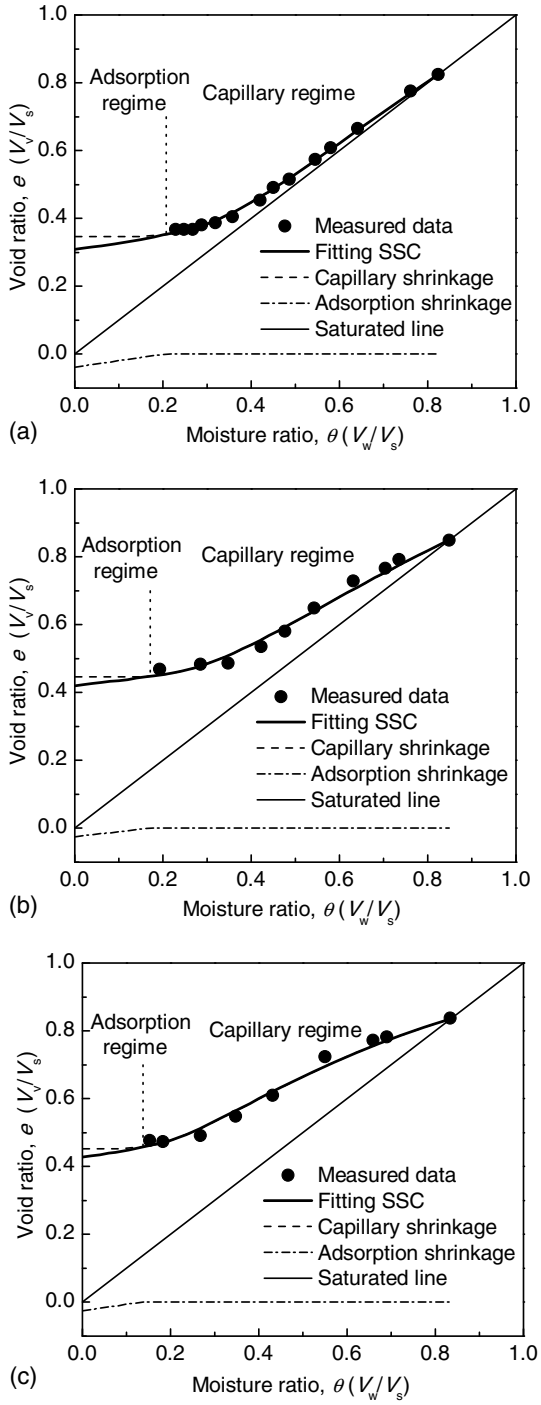

Fig. 2. Comparison of measured data and fitted SSC curves by proposed SSC equation for nonstructural and structural clayey soils: (a) Ragdale clay; (b) Faulkbourne Clay 1; and (c) Faulkbourne Clay 2. (Data from Reeve and Hall 1978.)

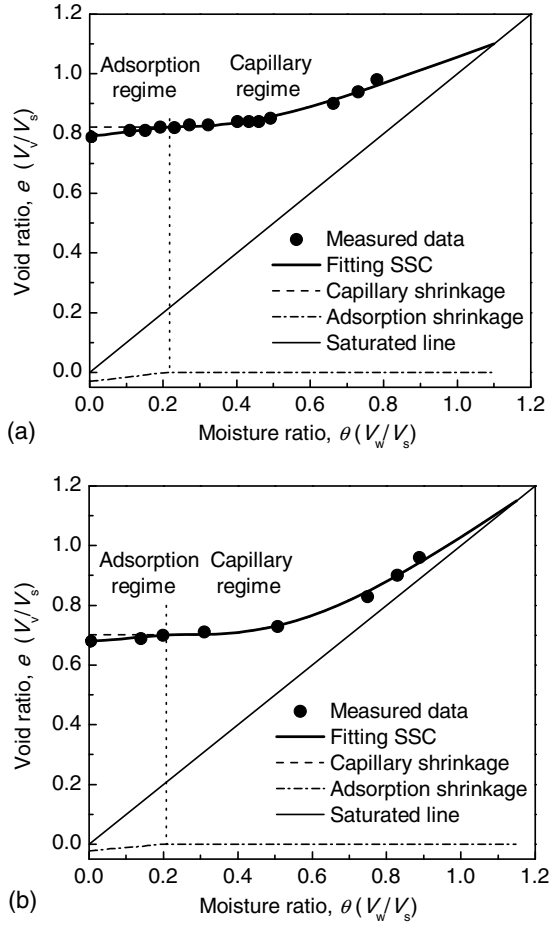

Fig. 3. Comparison of measured data and fitted SSC curves by proposed SSC equation for two soils: (a) Norwegian Clay 1; and (b) Norwegian Clay 2. (Data from Olsen and Haugen 1998.)

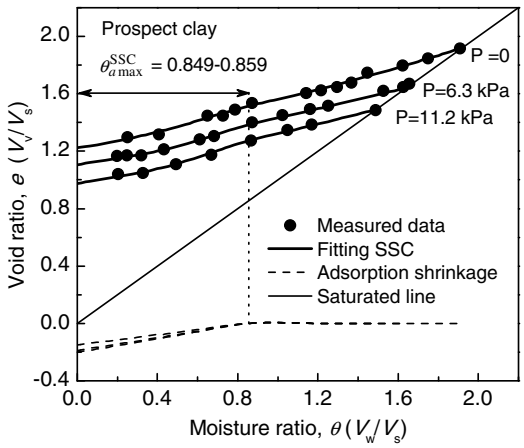

Fig. 4. Determination of maximum adsorption moisture ratio of identical expansive clay under various preloaded pressures by proposed SSC equation. (Data from Talsam 1977.)

Determining Maximum Adsorption Moisture Ratio of Clayey Soil

The proposed SSC equation introduces the maximum adsorption moisture ratio $\theta_{a\max}^{SSC}$ as an important parameter to distinguish adsorption and capillary shrinkage. One way to assess the proposed SSC equation is to determine whether the predicted maximum adsorption moisture ratio would be the same for the same soil but with different initial saturated void ratios or total stress conditions. Fig. 4 shows the SSC data for three pastes with different initial void ratios (Talsam 1977), together with the fitted SSCs by the proposed SSC equation. Table 2 lists the determined parameters of the SSC equation. The results show that the proposed SSC matched the measured data very well, with the coefficients of correlation all greater than 0.99 (Table 2). The preloaded pressures had little effect on the determined maximum adsorption moisture content $\theta_{a\max}^{SSC}$, which fell

in a narrow range of 0.849–0.859. The fact that the proposed SSC equation can identify very similar values of the maximum adsorption moisture content from these three apparently different SSCs of the same soil indicates the effectiveness of the proposed SSC equation in representing soil volume shrinkage due to adsorption and capillary water retention mechanisms. Furthermore, the fitted adsorption shrinkage rate gradually increased with the increase in the preloaded pressure, implying that the adsorption shrinkage rate is not only controlled by soil type but also affected by soil structure or stress history.

Determining Adsorption Moisture Ratio by Generalized SWRC Equation

To date, no experimental technique can directly quantify the capillary and adsorption water in soils. Hence, it is difficult to experimentally validate the maximum adsorption water content determined by the proposed SSC equation. Recently, Lu (2016) developed a generalized SWRC equation which can explicitly and quantitatively distinguish the water content between adsorption and capillary water. Hence, this study used the generalized SWRC model to determine the maximum adsorption water content of the soils by fitting the measured SWRC data from the literature (Dong and Lu 2016, 2017). The same soil specimen was used to determine the SWRC and SSC for each type of soil in the experiments. The effect of soil shrinkage on the SWRC was considered in determining the SWRCs of the four soils (Dong and Lu 2016, 2017).

Figs. 5(a)–7(a) show the SWRC data of the three soils. A brief description of Lu's (2016) SWRC model is provided here. Based on the local energy equilibrium principle, the total moisture ratio $\theta(\psi)$ is considered as a function of soil suction ψ, and can be divided into two parts: capillary moisture ratio $\theta_c(\psi)$, and adsorption moisture ratio $\theta_a(\psi)$, that is

$$\theta(\psi) = \theta_c(\psi) + \theta_a(\psi) \tag{6}$$

By introducing the cavitation concept, the capillary moisture ratio can be described as

$$\theta_c(\psi) = \frac{1}{2}\left[1 - \text{erf}\left(\sqrt{2}\frac{\psi - \psi_c}{\psi_c}\right)\right](\theta_s - \theta_a(\psi))[1 + (\alpha\psi)^n]^{-(1-1/n)} \tag{7}$$

where ψ_c = mean cavitation suction; θ_s = saturated moisture ratio; α is related to the inverse of air-entry suction; and n is related to pore-size distribution.

By considering the adsorption characteristics, and physical constraints, the adsorption moisture ratio can be described as

$$\theta_a(\psi) = \theta_{a\times\max}^{\text{SWRC}}\left\{1 - \left[\exp\left(\frac{\psi - \psi_{\max}}{\psi}\right)\right]^m\right\} \tag{8}$$

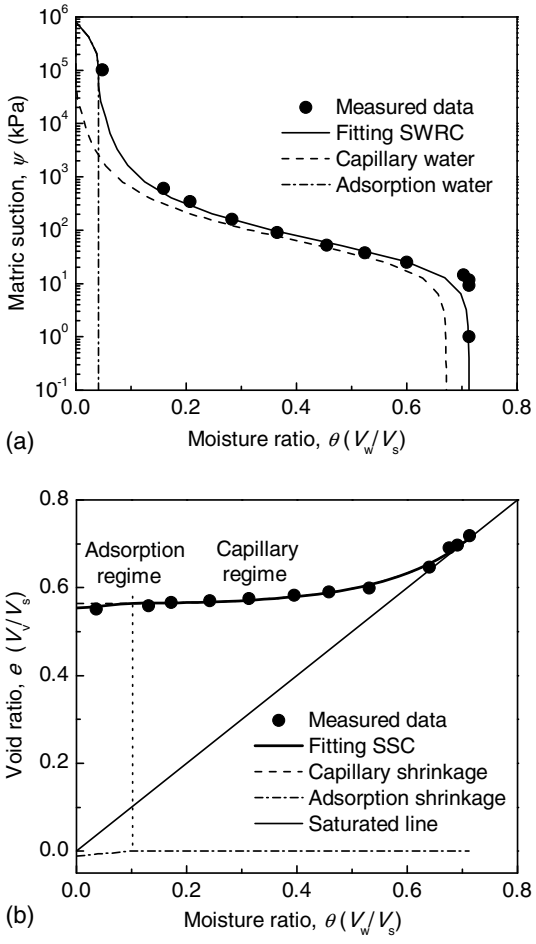

Fig. 5. Comparison of measured data and fitted SWRC by generalized SWRC equation of Lu (2016) and proposed SSC equation for Bonny silt: (a) SWRC (data from Dong and Lu 2016, 2017); and (b) SSC (data from Lu and Dong 2017).

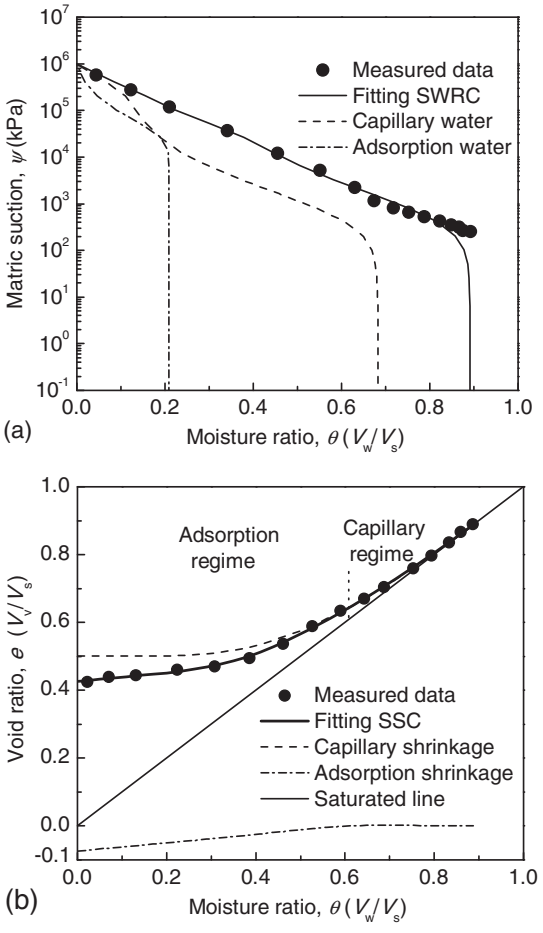

Fig. 6. Comparison of measured data and fitted SWRC by generalized SWRC equation of Lu (2016) and proposed SSC equation for Denver claystone: (a) SWRC (data from Dong and Lu 2016, 2017); and (b) SSC (data from Lu and Dong 2017).

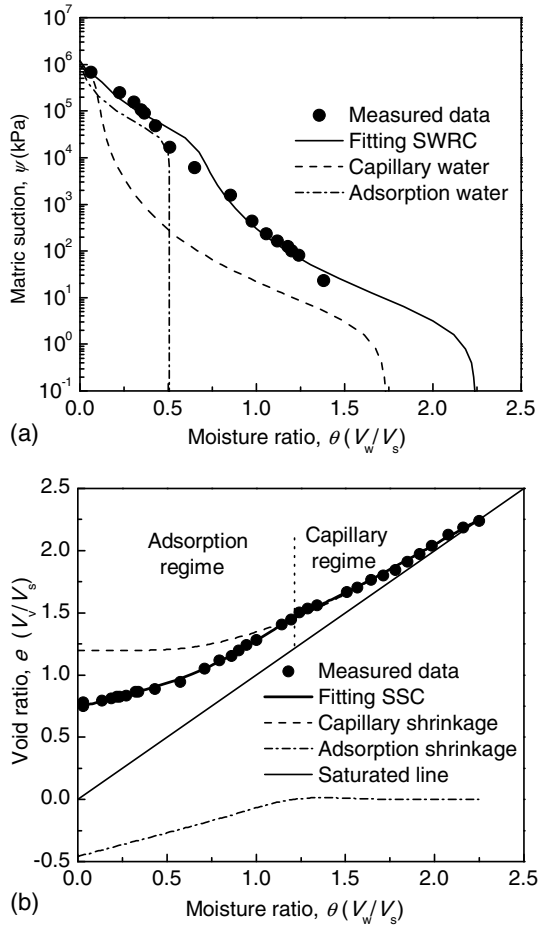

Fig. 7. Comparison of measured data and fitted SWRC by generalized SWRC equation of Lu (2016) and proposed SSC equation for Denver bentonite: (a) SWRC (data from Dong and Lu 2016, 2017); and (b) SSC (data from Lu and Dong 2017).

where $\theta_{a\times\max}^{\mathrm{SWRC}}$ = maximum adsorption water content; m = adsorption strength; and $\psi_{\max}$ = highest suction of soil. Eqs. (6)–(8) completely describe the SWRC in the full water content range with a total of seven parameters. Eqs. (6)–(8) were used to fit the SWRC data of the four soils, and Figs. 5(a)–7(a) show the fitted SWRCS. Table 3 lists the fitted SWR parameters and the coefficients of correlation.

Predicting Soil Shrinkage Behavior under Full Water Content Range

The proposed SSC equation was used to fit the experimental SSC data. Table 4 lists the fitted parameters and the correlation coefficients. Comparison of the measured SSC data and the predicted SSCs is shown in Fig. 5(b) for nonexpansive soils (Bonny silt) and in Figs. 6(b) and 7(b) for expansive clays (Denver claystone and Denver bentonite).

Figs. 5(b)–7(b) demonstrate that the predicted SSCs for all four soils matched the measured data well, including under very low moisture ratio range. Figs. 5(b)–7(b) also show the adsorption and capillary shrinkage. The soil shrinkage behavior varies greatly due to the control of capillary and adsorption water in different water content regimes for nonexpansive and expansive soils. For silty soil (Bonny silt) [Fig. 5(b)], the effect of adsorption water on the soil shrinkage was limited, due to the presence of relatively small adsorption water in these soils. This was also well reflected by the relatively small shrinkage rate in the adsorption regime ($c = 0.104$).

Unlike the shrinkage behavior of nonexpansive soils, the maximum decrease in the void ratio caused by the adsorption water [Figs. 6(b) and 7(b)] was 0.07 for the moderate expansive clay (Denver claystone) and 0.46 for the highly expansive clay (Denver bentonite). Compared with the nonexpansive soils, the expansive clays had much larger adsorption shrinkage rates (Table 4). This can be attributed to the higher adsorption water content (e.g., Lu 2016) and higher cation exchange capacity in the expansive clays (Table 1), leading to a significant shrinkage of the total void ratio [Figs. 6(b) and 7(b)].

Fig. 8(a) shows the correlation between the maximum adsorption moisture ratios obtained independently from the SWR and SSC data for the five examined soils. A linear relationship of 2.47:1 ratio between $\theta_{a\max}^{\mathrm{SSC}}$ and $\theta_{a\max}^{\mathrm{SWRC}}$ is clearly demonstrated, indicating that they are highly correlated ($R^2 = 0.99$) but are different in ranges. SWRC reflects the energy equilibrium between soil and water, whereas SSC reflects the mechanical (interparticle forces) equilibrium among soil particles. For the SWR, the adsorption water and capillary water have the same chemical potential in the overlapping or transition zone. The observed earlier onset of

Table 3. Fitted model parameters for generalized SWRC equation (Lu 2016) and corresponding coefficient of correlation for examined soils

Soil	θ_s	α (kPa^{-1})	n	ψ_c (MPa)	m	$\psi_{\max}$ (MPa)	$\theta_{a\max}^{\mathrm{SWRC}}$	R^2
Bonny silt	0.719	0.028	1.659	25	0.900	800	0.041	0.99
Iowa silt	0.968	0.149	1.513	6	0.170	580	0.041	0.99
BALT silt	0.850	0.083	1.500	50	0.800	600	0.091	1.00
Denver claystone	0.890	0.002	1.351	500	0.065	1,000	0.209	0.99
Denver bentonite	2.250	0.322	1.276	707	0.049	1,200	0.507	0.99

Table 4. Fitted model parameters for SSC equation and corresponding coefficients of correlation for examined soils

Soil	e_s	e_{c0}	β	η	c	$\theta_{a\max}^{\mathrm{SSC}}$	R^2
Bonny silt	0.719	0.564	2.080	2.335	0.104	0.102	0.99
Iowa silt	0.968	0.811	22.028	0.420	0.113	0.220	0.99
BALT silt	0.850	0.797	15.587	0.664	0.104	0.100	0.99
Denver claystone	0.890	0.501	0.084	26.355	0.122	0.608	1.00
Denver bentonite	2.250	1.198	0.077	22.015	0.378	1.213	1.00

J. Geotech. Geoenviron. Eng., 2018, 144(8): 04018046

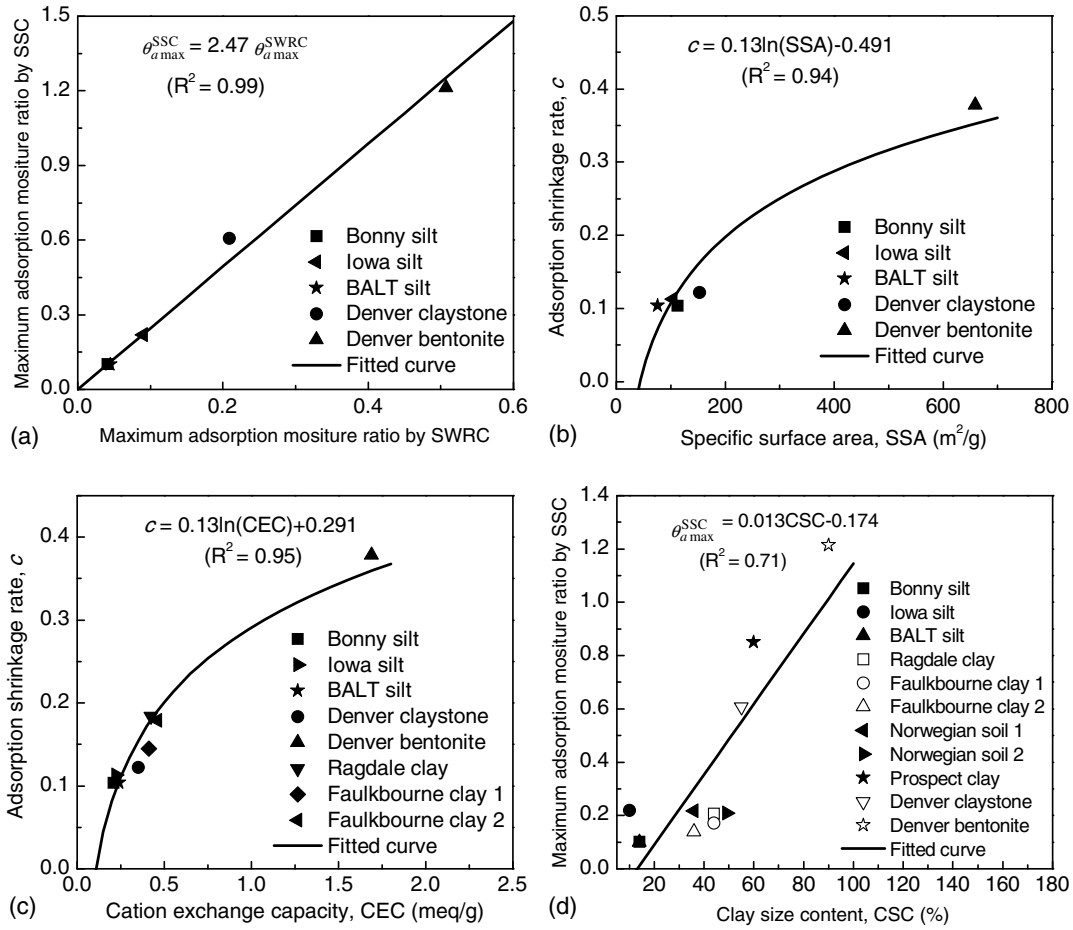

Fig. 8. (a) Correlation of fitted maximum adsorption moisture ratios by SWRC and by SSC equation for four examined soils; (b) correlation of adsorption shrinkage rate with specific surface area; (c) correlation of adsorption shrinkage rate with cation exchange capacity (data from Khorshidi et al. 2017; Khorshidi and Lu 2017b); and (d) correlation of maximum adsorption moisture ratios by SSC with clay-size content.

the mechanical effect indicates that capillary water in this transition zone acts mechanically similar to the adsorption water near the interparticle contacts.

Correlation between SSC and Physicochemical Indexes

Based on the preceding analysis, the adsorption shrinkage rate should have strong correlations with the SWR characteristics of SSA and CEC. This was confirmed by plotting the adsorption shrinkage rate as a function of the SSA of five of the examined soils [Fig. 8(b)] and as a function of the CEC of the examined soils [Fig. 8(c)]. The adsorption shrinkage rate increased as the SSA and CEC increased. The high correlations between the adsorption shrinkage rate and SSA ($R^2 = 0.94$) and between the adsorption shrinkage rate and CEC ($R^2 = 0.95$) indicate that the soil volume shrinkage due to the loss of moisture ratio in the low moisture ratio is mainly controlled by the particle dehydration, including both surface and cation dehydration.

Furthermore, the same exponential form between the fitted adsorption shrinkage rate c and SSA and between the fitted adsorption shrinkage rate and CEC was revealed for silty and for clayey soils [Figs. 8(b and c)]. Lu and Dong (2017) identified the same exponential form between the measured adsorption shrinkage rate and SSA and between the measured adsorption shrinkage rate and CEC. The present finding confirms the validity of the conception of the proposed SSC in representing soil volume shrinkage due to the water adsorption mechanism.

The correlation of the maximum adsorption moisture ratio by the proposed SSC equation $\theta_{a\max}^{SSC}$ with the clay-size content of all the examined soils also was explored. Fig. 8(d) shows a linear relationship between $\theta_{a\max}^{SSC}$ and CSC, with $R^2 = 0.71$. Therefore, it is possible to estimate a soil's $\theta_{a\max}^{SSC}$ parameter from its soil classification.

Summary and Conclusions

Considering the mechanical effect of soil-water interaction of capillary and adsorption water on the volume shrinkage of clayey soils, a new SSC model was established. The main conclusions and suggestions are as follows:

1. The novel feature of the proposed SSC, compared with all previous SSC models and theories, is the inclusion of the nonzero shrinkage behavior in the low moisture ratio or water content. A closed-form SSC equation in the full water content range was proposed, which decomposes shrinkage volume into two superimposable components: a linear relation for adsorption shrinkage, and a sigmoid relation for capillary shrinkage.
2. The measured soil shrinkage data from the literature for a variety of soils were used to assess the effectiveness of the proposed SSC equation. The results showed that the proposed SSC equation performs very well in the full water content range. The proposed SSC equation generalizes the soil shrinkage behavior

because it is capable of charactering the soil volume shrinkage for soils with both nonzero and zero adsorption shrinkage rates.

3. The concept of the maximum adsorption moisture ratio θ_{amax}^{SSC} was further examined through an expansive soil with different structures and preloaded pressures. The results showed that parameter θ_{amax}^{SSC} can be considered as an intrinsic parameter of a soil because it is independent of the initial structure and applied pressures. A strong correlation between the maximum adsorption moisture ratios obtained independently from the SWR and SSC data was found and a linear relationship of a 2.47:1 ratio between θ_{amax}^{SSC} and θ_{amax}^{SWRC} was clearly delineated. The earlier onset of the mechanical effect due to adsorption indicates that capillary water in the transition zone acts mechanically similar to the adsorption water.
4. The correlation of the adsorption shrinkage rate with the SWR characteristics was examined. The adsorption shrinkage rate was shown to be highly correlated with the SWR characteristics of SSA and CEC. The same exponential form between the fitted adsorption shrinkage rate and the SWR characteristics was found, confirming the previous discovery for the same exponential form between the measured adsorption shrinkage rate and the SWR characteristics. This implies that an intrinsic relationship exists between a soil's SSA and CEC. A linear correlation of the maximum adsorption moisture ratio and the clay-size content was found, implying that the standard soil classification can be used as a basis for estimating the maximum adsorption moisture ratio for SSC.

Acknowledgments

This research is supported by the US National Science Foundation (Grant Nos. CMMI 1233063 and CMMI 1230544), and the National Natural Science Foundation of China (Grant No. 11302243). The first author is also supported by the Chinese Academy of Science for overseas study.

References

Assi, A., J. Accola, G. Hovhannissian, R. H. Mohtar, and E. Braudeau. 2014. "Physics of the soil medium organization. Part 2: Pedostructure characterization through measurement and modeling of the soil moisture characteristic curves." *Front. Environ. Sci.* 2 (5): 1–17. https://doi.org/10.3389/fenvs.2014.00005.

Boivin, P., P. Garnier, and D. Tessier. 2004. "Relationship between clay content, clay type, and shrinkage properties of soil samples." *Soil Sci. Soc. Am. J.* 68 (4): 1145–1153. https://doi.org/10.2136/sssaj2004.1145.

Boivin, P., P. Garnier, and M. Vauclin. 2006. "Modeling the soil shrinkage and water retention curves with the same equations." *Soil Sci. Soc. Am. J.* 70 (4): 1082–1093. https://doi.org/10.2136/sssaj2005.0218.

Braudeau, E., J. M. Costantini, G. Bellier, and H. Colleuille. 1999. "New device and method for soil shrinkage curve measurement and characterization." *Soil Sci. Soc. Am. J.* 63 (3): 525–535. https://doi.org/10.2136/sssaj1999.03615995006300030015x.

Braudeau, E., M. Sene, and R. H. Mohtar. 2005. "Hydrostructural characteristic of two African tropical soils." *Eur. J. Soil Sci.* 56 (3): 375–388. https://doi.org/10.1111/j.1365-2389.2004.00679.x.

Chertkov, V. Y. 2003. "Modelling the shrinkage curve of soil clay pastes." *Geoderma* 112 (1–2): 71–95. https://doi.org/10.1016/S0016-7061(02)00297-5.

Cornelis, W. M., J. Corluy, H. Medina, J. Diaz, R. Hartmann, M. Van Meirvenne, and M. E. Ruiz. 2006. "Measuring and modelling the soil shrinkage characteristic curve." *Geoderma* 137 (1–2): 179–191. https://doi.org/10.1016/j.geoderma.2006.08.022.

Crescimanno, G., and G. Provenzano. 1999. "Soil shrinkage characteristic curve in clay soils: Measurement and prediction." *Soil Sci. Soc. Am. J.* 63 (1): 25–32. https://doi.org/10.2136/sssaj1999.03615995006300010005x.

Dong, Y., and N. Lu. 2016. "Correlation between small-strain shear modulus and suction stress in capillary regime under zero total stress conditions." *J. Geotech. Geoenviron. Eng.* 142 (11): 04016056. https://doi.org/10.1061/(ASCE)GT.1943-5606.0001531.

Dong, Y., and N. Lu. 2017. "Measurement of suction-stress characteristic curve under drying and wetting conditions." *Geotech. Test. J.* 40 (1): 1–15. https://doi.org/10.1520/GTJ20160058.

Fredlund, M. D., G. W. Wilson, and D. G. Fredlund. 2002. "Representation and estimation of the shrinkage curve." In *Proc., 3rd Int. Conf. on Unsaturated Soils (UNSAT 2002)*, edited by De C. Jucá and Marinho, 145–149. Lisse, Netherlands: Swets and Zeitlinger .

Groenevelt, P. H., and G. H. Bolt. 1972. "Water retention in soil." *Soil Sci.* 113 (4): 238–245. https://doi.org/10.1097/00010694-197204000-00003.

Haines, W. B. 1923. "The volume-changes associated with variations of water content in soil." *J. Agric. Sci.* 13 (3): 296–310. https://doi.org/10.1017/S0021859600003580.

Khorshidi, M., and N. Lu. 2017a. "Determination of cation exchange capacity from soil water retention curve." *J. Eng. Mech.* 143 (6): 04017023. https://doi.org/10.1061/(ASCE)EM.1943-7889.0001220.

Khorshidi, M., and N. Lu. 2017b. "Intrinsic relation between soil water retention and cation exchange capacity." *J. Geotech. Geoenviron. Eng.* 143 (4): 04016119. https://doi.org/10.1061/(ASCE)GT.1943-5606.0001633.

Khorshidi, M., N. Lu, I. Akin, and W. Likos. 2017. "Intrinsic relationship between specific surface area and soil water retention." *J. Geotech. Geoenviron. Eng.* 143 (1): 04016078. https://doi.org/10.1061/(ASCE)GT.1943-5606.0001572.

Kim, D. J., H. Vereecken, J. Feyen, D. Boels, and J. J. B. Bronswijk. 1992. "On the characterization of properties of an unripe marine clay soil. I: Shrinkage processes of an unripe marine clay soil in relation to physical ripening." *Soil Sci.* 153 (6): 471–481. https://doi.org/10.1097/00010694-199206000-00006.

Leong, E. C., and M. Wijaya. 2015. "Universal soil shrinkage curve equation." *Geoderma* 237–238 (Jan): 78–87. https://doi.org/10.1016/j.geoderma.2014.08.012.

Likos, W. J., and N. Lu. 2003. "Automated humidity system for measuring total suction characteristics of clay." *Geotech. Test. J.* 26 (2): 1–12. https://doi.org/10.1520/GTJ10456262.

Lu, N. 2016. "Generalized soil water retention equation for adsorption and capillarity." *J. Geotech. Geoenviron. Eng.* 142 (10): 04016051. https://doi.org/10.1061/(ASCE)GT.1943-5606.0001524.

Lu, N., and Y. Dong. 2017. "Correlation between soil shrinkage curve and water retention characteristics." *J. Geotech. Geoenviron. Eng.* 143 (9): 04017054. https://doi.org/10.1061/(ASCE)GT.1943-5606.0001741.

Lu, N., and M. Kaya. 2013. "A drying cake method for measuring suction stress characteristic curve, soil-water retention, and hydraulic conductivity function." *Geotech. Test. J.* 36 (1): 1–19. https://doi.org/10.1520/GTJ20120097.

Lu, N., and M. Kaya. 2014. "Power law for elastic moduli of unsaturated soil." *J. Geotech. Geoenviron. Eng.* 140 (1): 46–56. https://doi.org/10.1061/(ASCE)GT.1943-5606.0000990.

Lu, N., and M. Khorshidi. 2015. "Mechanism for soil-water retention and hysteresis at high suction range." *J. Geotech. Geoenviron. Eng.* 141 (8): 04015032. https://doi.org/10.1061/(ASCE)GT.1943-5606.0001325.

Lu, N., and W. J. Likos. 2006. "Suction stress characteristic curve for unsaturated soil." *J. Geotech. Geoenviron. Eng.* 132 (2): 131–142. https://doi.org/10.1061/(ASCE)1090-0241(2006)132:2(131).

Mathews, J., and R. L. Walker. 1970. *Mathematical methods of physics*. Vol. 501. New York: WA Benjamin.

McGarry, D., and I. G. Daniells. 1987. "Shrinkage curve indices to quantify cultivation effects on soil structure of a vertisol." *Soil Sci. Soc. Am. J.* 51 (6): 1575–1580. https://doi.org/10.2136/sssaj1987.03615995005100060031x.

McGarry, D., and K. W. J. Malafant. 1987. "The analysis of volume change in unconfined units of soil." *Soil Sci. Soc. Am. J.* 51 (2): 290–297. https://doi.org/10.2136/sssaj1987.03615995005100020005x.

Millette, J. A., and R. S. Broughton. 1984. "The effect of water table in organic soil on subsidence and swelling." *Can. J. Soil Sci.* 64 (2): 273–282. https://doi.org/10.4141/cjss84-028.

Mitchell, A. R. 1992. "Shrinkage terminology: Escape from 'normalcy'." *Soil Sci. Soc. Am. J.* 56 (3): 993–994. https://doi.org/10.2136/sssaj1992.03615995005600030053x.

Olsen, P. A., and L. E. Haugen. 1998. "A new model of the shrinkage characteristic applied to some Norwegian soils." *Geoderma* 83 (1–2): 67–81. https://doi.org/10.1016/S0016-7061(97)00145-6.

Peng, X., and R. Horn. 2005. "Modeling soil shrinkage curve across a wide range of soil types." *Soil Sci. Soc. Am. J.* 69 (3): 584–592. https://doi.org/10.2136/sssaj2004.0146.

Peng, X., and R. Horn. 2013. "Identifying six types of soil shrinkage curves from a large set of experimental data." *Soil Sci. Soc. Am. J.* 77 (2): 372–381. https://doi.org/10.2136/sssaj2011.0422.

Reeve, M. J., and D. G. M. Hall. 1978. "Shrinkage in clayey subsoils of contrasting structure." *J. Soil Sci.* 29 (3): 315–323. https://doi.org/10.1111/j.1365-2389.1978.tb00779.x.

Sridharan, A., and G. V. Rao. 1971. "Effective stress theory of shrinkage phenomena." *Can. Geotech. J.* 8 (4): 503–513. https://doi.org/10.1139/t71-052.

Talsam, T. 1977. "A note on the shrinkage behaviour of a clay paste under various loads." *Aust. J. Soil Res.* 15 (3): 275–277. https://doi.org/10.1071/SR9770275.

Tariq, A. U. R., and D. S. Durnford. 1993. "Analytical volume change model for swelling clay soils." *Soil Sci. Soc. Am. J.* 57 (5): 1183–1187. https://doi.org/10.2136/sssaj1993.03615995005700050003x.

Tempany, H. A. 1917. "The shrinkage of soils." *J. Agric. Sci.* 8 (3): 312–330. https://doi.org/10.1017/S0021859600002951.

van Genuchten, M. T. 1980. "A closed form equation for predicting the hydraulic conductivity of unsaturated soils." *Soil Sci. Soc. Am. J.* 44 (5): 892–898. https://doi.org/10.2136/sssaj1980.03615995004400050002x.

White, D. J., W. A. Take, and M. D. Bolton. 2003. "Soil deformation measurement using particle image velocimetry (PIV) and photogrammetry." *Geotechnique* 53 (7): 619–631. https://doi.org/10.1680/geot.2003.53.7.619.

Wijaya, M., E. C. Leong, and H. Rahardjo. 2015. "Effect of shrinkage on air-entry value of soils." *Soils Found.* 55 (1): 166–180. https://doi.org/10.1016/j.sandf.2014.12.013.

Zolfaghari, Z., M. R. Mosaddeghi, and S. Ayoubi. 2016. "Relationships of soil shrinkage parameters and indices with intrinsic soil properties and environmental variables in calcareous soils." *Geoderma* 277 (Sep): 23–34. https://doi.org/10.1016/j.geoderma.2016.04.022.